

## Lattice solitons with quadrupolar intersite interactions

Yongyao Li,<sup>1,2,3</sup> Jingfeng Liu,<sup>1</sup> Wei Pang,<sup>4</sup> and Boris A. Malomed<sup>2,\*</sup>

<sup>1</sup>*Department of Applied Physics, South China Agricultural University, Guangzhou 510642, China*

<sup>2</sup>*Department of Physical Electronics, School of Electrical Engineering, Faculty of Engineering, Tel Aviv University, Tel Aviv 69978, Israel*

<sup>3</sup>*Modern Educational Technology Center, South China Agricultural University, Guangzhou 510642, China*

<sup>4</sup>*Department of Experiment Teaching, Guangdong University of Technology, Guangzhou 510006, China*

(Received 18 November 2013; published 23 December 2013)

We study two-dimensional (2D) solitons in the mean-field models of ultracold gases with long-range quadrupole-quadrupole interaction (QQI) between particles. The condensate is loaded into a deep optical-lattice (OL) potential, therefore the model is based on the 2D discrete nonlinear Schrödinger equation with contact on site and long-range intersite interactions, which represent the QQI. The quadrupoles are built as pairs of electric dipoles and antidipoles orientated perpendicular to the 2D plane to which the gas is confined. Because the quadrupoles interact with the local gradient of the external field, they are polarized by an inhomogeneous dc electric field that may be supplied by a tapered capacitor. Shapes, stability, mobility, and collisions of fundamental discrete solitons are studied by means of systematic simulations. In particular, threshold values of the norm, which are necessary for the existence of the solitons, are found and anisotropy of their static and dynamical properties is explored. As concerns the mobility and collisions, we analyze such properties for discrete solitons on 2D lattices with long-range intersite interactions. Estimates demonstrate that the setting can be realized under experimentally available conditions, predicting solitons built of  $\sim 10\,000$  particles.

DOI: [10.1103/PhysRevA.88.063635](https://doi.org/10.1103/PhysRevA.88.063635)

PACS number(s): 03.75.Lm, 05.45.Yv, 63.20.Ry, 47.11.Qr

### I. INTRODUCTION

Interactions between particles play a crucial role in the dynamics of Bose-Einstein condensates (BECs). Ubiquitous are short-range contact interactions, which are described by the single parameter: the  $s$ -wave scattering length  $a_s$  [1–3]. More specific are isotropic long-range Van der Waals interactions between Rydberg atoms in ultracold bosonic gases [4,5], and anisotropic long-range dipole-dipole interactions (DDIs) in dipolar condensates [6–11]. DDIs occur in gases formed by magnetic atoms, such as Cr, Dy, Er [12–14], or gases of molecules carrying electric dipole moments—for instance, CO, ND, and OH [15–17]. Using external dc magnetic or electric fields polarizing permanent atomic or molecular moments, plenty of controllable structures, including solitons, have been predicted and demonstrated in dipolar condensates [7,9,11,18–65]. Many such structures are supported by optical lattices (OLs). In the limit of deep OL potentials, the description of the dipolar BEC is provided by discrete models with long-range intersite interactions [27,28,32,36,37,41,43,51,59]. Moreover, it was predicted [60,61] and demonstrated experimentally [62] that the interaction of particles carrying permanent electric dipole moments with a singular dc field created by a charged wire or a point-like charge may give rise both to the specific collapse mechanism and to its suppression by interparticle interactions. In addition, the repulsive DDIs between moments induced by nonuniform dc fields in a gas of nondipolar polarizable particles may give rise to bright solitons of a completely different type [63].

In this work, we propose the possibility of formation of two-dimensional (2D) matter-wave solitons in nondipolar molecular ultracold gas, loaded into a deep OL potential, with long-range quadrupole-quadrupole interactions (QQIs) between particles. Experimental methods for the measurement

of molecular quadrupole moments are well elaborated [66]. It has been reported that some simple molecules, such as acetylene [67], have relatively large quadrupole moments ( $\simeq 6$  D Å). Still larger moments were measured in long-lived metastable states of alkaline-earth-metal [68,69] and ytterbium [70] atoms ( $\simeq 20$  D Å), and in alkaline diatoms [71] (up to  $\simeq 50$  D Å). As recently shown for fermions, such sizes for quadrupole moments are sufficient to generate new phases in quantum gases trapped in the OL [72]. Furthermore, it has been predicted that the QQI can be strongly amplified by means of optical vortices [73].

There are two straightforward settings, for electric and magnetic quadrupoles, which can feature QQIs in a 2D geometry. One relies upon electric quadrupoles, built as tightly bound pairs of dipoles and antidipoles, which are directed *perpendicular* to the system's plane ( $x, y$ ), i.e., along axis  $z$ . Because the quadrupole interacts with the gradient of the external field, rather than with the field itself, in this setting the quadrupoles may be aligned (polarized) by an external electric field which is also directed along  $z$ , and whose strength is a linearly growing function of  $x$ . Such an electric field can be imposed, in turn, by a *tapered capacitor*; see Fig. 1(a).

Quadrupoles (both electric and magnetic) are described by a symmetric traceless tensor  $Q_{\alpha\beta}$  ( $\alpha, \beta = x, y, z$ ) with  $\sum_{\alpha} Q_{\alpha\alpha} \equiv 0$  [74]. In this notation, the electric quadrupole defined above [in Fig. 1(a)] has the following components:

$$Q_{xy} = Q_{yx} \equiv Q, \quad Q_{zz} = Q_{zx} = Q_{xz} = Q_{yz} = 0, \quad (1)$$

where the quadrupole moment per se is defined as

$$Q = 3d\varepsilon, \quad (2)$$

with  $\pm d$  and  $\varepsilon$  being, respectively, the dipolar moments of the bound dipoles and antidipole and the distance between them.

The potential of the interaction between two quadrupoles of the present type in the planar configuration considered here can be derived from the general formula for the QQI potential

\*malomed@post.tau.ac.il

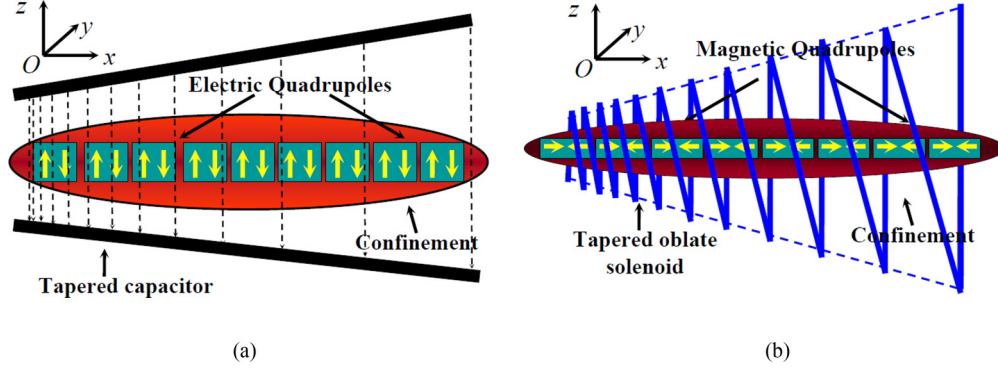


FIG. 1. (Color online) (a) Electric quadrupoles, built as tightly bound pairs of dipole and antidipoles directed perpendicular to the  $(x, y)$  plane. They are polarized by the dc electric field which is also directed along  $z$  and whose strength is a linear function of  $x$ . As shown here, the field can be imposed by a tapered capacitor. (b) Magnetic quadrupoles, built as tightly bound dipole-antidipole pairs directed along axis  $x$ . They can be aligned by means of the dc magnetic field directed along  $x$ , whose strength is a linear function of  $x$ . The magnetic field can be created by the tapered solenoid, as shown in panel (b).

[75], the result being

$$U_{\text{QQ}}^{(\text{electr})}(r, \theta) = \frac{4}{3} Q^2 r^{-5} (1 - 5 \cos^2 \theta), \quad (3)$$

where  $r$  is the distance between the quadrupoles, and  $\theta$  is the angle between the vector connecting the quadrupoles and the line connecting the dipole and antidipole inside the quadrupole (the latter direction is here defined as axis  $x$ ).

On the other hand, it is possible to introduce magnetic quadrupoles, built as tightly bound pairs of dipoles and antidipoles directed *in plane*, along axis  $x$ . Because these quadrupoles also interact with the gradient of the external field, they may be aligned by means of the magnetic field directed along  $x$ , whose strength grows linearly with  $x$ . This field may be applied by a *tapered oblate solenoid*; see Fig. 1(b). The respective quadrupole tensor is

$$Q_{yy} = Q_{zz} = -\frac{1}{2} Q_{xx}, \quad Q_{xy} = Q_{zx} = Q_{yz} = 0. \quad (4)$$

The potential of the interaction between the quadrupoles of the present type can also be derived from the general formula [75], yielding

$$U_{\text{QQ}}^{(\text{magn})}(r, \theta) = \frac{4}{3} Q^2 r^{-5} (3 - 30 \cos^2 \theta + 35 \cos^4 \theta). \quad (5)$$

Averaging potentials (3) and (5) over the entire angular range  $0 \leq \theta < 2\pi$  yields mean values which correspond to attraction and repulsion, respectively:

$$\frac{1}{2\pi} \int_0^{2\pi} U_{\text{QQ}}^{(\text{electr})}(R, \theta) d\theta = -2Q^2 r^{-5} < 0, \quad (6)$$

$$\frac{1}{2\pi} \int_0^{2\pi} U_{\text{QQ}}^{(\text{magn})}(R, \theta) d\theta = \frac{3}{2} Q^2 r^{-5} > 0. \quad (7)$$

Hence potential (3) has a chance to create 2D solitons, while for potential (5) this is not plausible. Indeed, numerical tests with interaction kernel (5) have not revealed soliton modes. Therefore, in what follows below we consider the model with the QQI defined as per Eq. (3) and Fig. 1(a).

For the sake of comparison, it is relevant to compare expression (3) and (5) with the commonly known potential of the DDI for a pair of in-plane-oriented parallel dipoles with moment  $D$ :

$$U_{\text{DD}}(r, \theta) = \frac{1}{3} D^2 r^{-3} (1 - 3 \cos^2 \theta). \quad (8)$$

Note that this potential is attractive, on average:

$$\frac{1}{2\pi} \int_0^{2\pi} U_{\text{DD}}(R, \theta) d\theta = -\frac{1}{6} D^2 r^{-3} < 0. \quad (9)$$

Accordingly, the existence of stable anisotropic 2D solitons in this setting was first demonstrated in Ref. [9].

The objective of this work is to study shapes, stability, mobility, and collisions of 2D matter-wave solitons in BECs formed by quadrupole particles trapped in a deep optical lattice (OL). The discrete model describing the present setting is derived in Sec. II, where we also present estimates of physical parameters of the setting and of the expected soliton states. Results of systematic numerical studies of static 2D solitons in the model are reported in Sec. III, and their dynamical properties; namely, mobility and collisions, are presented in Section IV. It is relevant to stress that mobility and collisions of 2D discrete solitons were not previously studied in any lattice system with long-range interactions. The paper is concluded by Sec. V.

## II. THE MODEL EQUATION

The underlying 3D Gross-Pitaevskii equation (GPE) [1], which takes into regard both the contact isotropic nonlinearity and the long-range QQI corresponding to potential (3), can be reduced to the normalized 2D equation,

$$0 = i \frac{\partial \psi}{\partial t} + \frac{1}{2} \left( \frac{\partial^2}{\partial x^2} + \frac{\partial^2}{\partial y^2} \right) \psi - g |\psi|^2 \psi - U(x, y) \psi - G \psi(\mathbf{r}) \int |\psi(\mathbf{r}')|^2 (1 - 5 \cos^2 \theta) \frac{d\mathbf{r}'}{|\mathbf{r} - \mathbf{r}'|^5}, \quad (10)$$

where  $\mathbf{r} \equiv \{x, y\}$ , angle  $\theta$  has the same meaning as in Eq. (3), and  $U(x, y)$  represents the OL potential. The derivation of Eq. (10) assumes the factorization of the three-dimensional (3D) mean-field wave function  $\Psi$  under the action of the tight trapping potential imposed in the transverse direction:

$$\Psi(X, Y, Z, T) = (\sqrt{\pi} a_{\perp}^3)^{-1/2} \exp \left( -\frac{i\hbar}{2m a_{\perp}^2} T - \frac{1}{2} Z^2 \right) \psi(x, y, t), \quad (11)$$

where the scaled coordinates and time are related to the physical ones  $X, Y, Z, T$  as follows:  $\{X, Y, Z\} \equiv a_{\perp}\{x, y, z\}$ ,  $T \equiv (ma_{\perp}^2/\hbar)t$ ,  $a_{\perp}$  is the transverse localization length, and  $m$  is the mass of the particle. As it follows from the factorized ansatz (11), the total number of particles in the condensate is given by

$$P_{\text{total}} = \iint |\psi(x, y)|^2 dx dy. \quad (12)$$

The rescaling implied above gives rise to expressions for dimensionless coefficients of the contact and long-range interactions in Eq. (10) in terms of the scattering length  $a_s$  and quadrupole moment:

$$g = 2\sqrt{2\pi} \frac{a_s}{a_{\perp}}, \quad G = \frac{4mQ^2}{3\hbar^2 a_{\perp}^3}. \quad (13)$$

Equation (10) belongs to the class of nonlocal nonlinear Schrödinger (NLS) equations which, unlike their local counterpart with the self-attractive cubic term, are free of collapse in the 2D geometry [76,77], therefore 2D solitons are stable in such models, contrary to the commonly known instability of Townes solitons in the local 2D NLS equation [78]. Furthermore, the nonlocality affects the character of the interaction between 2D solitons. In particular, interactions between dark solitons and between out-of-phase bright modes can be made attractive, in contrast with the repulsion in local models; see a brief review [77] for nonlocal NLS equations in models of nonlinear optics.

The next step is to replace the continuous equation (10) by its discrete counterpart, corresponding to the condensate fragmented by a deep OL potential. To this end, the continuous wave function is decomposed over a set of modes strongly localized in vicinity of each OL site (Wannier functions),

$$\psi(x, y, t) = \sum_{m,n} \psi_{mn}(t) \Phi_{mn}(x, y), \quad (14)$$

where  $m, n$  are discrete coordinates on the lattice, as was done in the course of the derivation of the one-dimensional (1D) [27] and 2D [36] discrete models for the dipolar BEC trapped in deep OL potentials. The result is the following rescaled discrete version of Eq. (10), i.e., a 2D discrete NLS equation with long-range interactions:

$$\begin{aligned} \partial_t \psi_{mn} = & -\frac{1}{2}(\psi_{m+1,n} + \psi_{m-1,n} + \psi_{m,n+1} + \psi_{m,n-1} - 4\psi_{mn}) \\ & + \sigma |\psi_{mn}|^2 \psi_{mn} \\ & + \psi_{mn} \sum_{\{m',n'\} \neq \{m,n\}} f_{\text{QQ}}(m-m', n-n') |\psi_{m'n'}|^2, \end{aligned} \quad (15)$$

with the discrete QQI kernel,

$$f_{\text{QQ}}(m-m', n-n') = \frac{(n-n')^2 - 4(m-m')^2}{[(m-m')^2 + (n-n')^2]^{7/2}}. \quad (16)$$

The rescaling is performed here in the same way as was done in Ref. [36]; namely, by using coefficients which are expressed in the form of normalization and overlapping integrals built of the Wannier functions. Note that the coefficient in front of the QQI terms is scaled here to be 1, while  $\sigma$  is the relative strength

of the contact interactions. Obviously, Eq. (15) conserves the norm of the discrete wave function, which is the discrete counterpart of the norm (12):

$$P = \sum_{m,n} |\psi_{mn}|^2. \quad (17)$$

It is well known that the discretization of the NLS equation is another general mechanism helping to suppress the collapse and ensuing instability of solitons in the 2D NLS equation [79]. Likewise, the discreteness readily stabilizes 2D discrete solitons with embedded vorticity [80]. Furthermore, it was demonstrated both theoretically and experimentally that stable 2D gap solitons are supported by a system modeled by the discrete NLS equation with long-range intersite interactions [81]. It is relevant to mention too that, in addition to its realizations in optics and BECs, the discrete NLS equation with long-range intersite interactions models the so-called Scheibe aggregates of closely packed molecules, in which soliton solutions are known as well [82].

The analysis reported below is based on Eq. (15). Note that the discrete equation which was derived in Refs. [36,37] for the dipolar BEC trapped in the deep OL potential differs by the form of the interaction kernel, which is the discrete counterpart of the DDI kernel (8):

$$f_{\text{DD}}(m-m', n-n') = \frac{(n-n')^2 - 2(m-m')^2}{[(m-m')^2 + (n-n')^2]^{5/2}}. \quad (18)$$

It is also relevant to mention that Eq. (15) with  $\sigma = 0$  applies as well to fermion lattice gases with the long-range interaction; cf. Ref. [72].

Finally, to estimate the range of physical parameters allowing the implementation of the present model, the magnitude of the quadrupole moment can be estimated for a complex built as a square with charges  $(+e, -e, +e, -e)$  set at its vertices, with linear size  $\varepsilon$  ( $e$  is the electron's charge). According to Eq. (2), the corresponding quadrupole momentum is

$$Q = 3e\varepsilon^2. \quad (19)$$

Then, adopting typical values  $a_s \simeq 5$  nm,  $a_{\perp} \simeq 1$   $\mu$ m, and  $m \simeq 100$  proton masses, Eqs. (10), (13), and (3) can be used to estimate the linear size of the quadrupole,  $\varepsilon$ , which is necessary to make the strength of the QQI comparable to that of the contact interactions. The result is  $\varepsilon \sim 1$  nm, which is quite realistic for small molecules. Furthermore, typical scaled characteristics of solitons reported below, if translated back into physical units, lead to an estimate  $\sim 30$   $\mu$ m for the linear size of 2D solitons built of  $\sim 10\,000$  particles.

### III. NUMERICAL RESULTS

#### A. Shape and stability of the solitons

Stationary solutions to Eq. (15) with real chemical potential  $\mu$  were looked for in the usual form

$$\psi_{mn}(t) = \phi_{mn} e^{-i\mu t}. \quad (20)$$

Stationary profiles  $\phi_{mn}$  were found in a finite domain of size  $N \times N$  by means of the well-known imaginary-time propagation method [83–85]. The stability of the so-found solitons was then tested by simulations of their evolution in

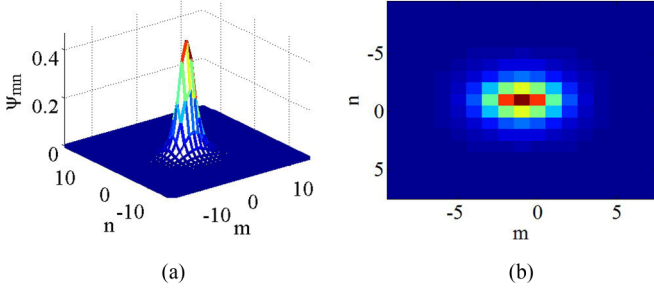


FIG. 2. (Color online) Side (a) and top (b) views of a stable discrete soliton supported by the long-range quadrupole interactions. The soliton was found as a stationary solution of Eq. (15) with  $\sigma = 0$  (no contact interactions) and norm  $P = 1.2$ , on the lattice of size  $32 \times 32$ . In this case,  $P_{cr} = 0.86$ ; see Fig. 3(b).

real time, adding random perturbations to the initial conditions. It is instructive to present the results for solitons maintained by the QQI, comparing them to those obtained in the model with the DDI kernel (8) in Refs. [36,37].

For both models QQI and DDI, the numerical results reveal a critical value of the norm,  $P_{cr}$ , below which discrete wave packets do not self-trap into 2D solitons but rather spread out into almost flat states via the delocalization transition, which is a generic feature of 2D systems [86]. In fact,  $P_{cr}$  originates from the norm of the *Townes soliton*, which is the single value at which the degenerate family of solitons exist in the uniform 2D medium with the self-attractive local cubic nonlinearity [87], and which is stretched into a finite existence interval under the stabilizing action of the OL potential [88]. We have found that all the solitons existing at  $P > P_{cr}$  are stable.

A typical example of a discrete soliton maintained by the QQI nonlinearity is displayed in Fig. 2. As expected, the soliton's shape is anisotropic, being prolate in the  $m$  direction, in accordance with the fact that the QQI kernel (16) is attractive along  $m$  and repulsive in the perpendicular direction.

As shown in Figs. 3(a)–3(c) for different fixed values of strength  $\sigma$  of the contact nonlinearity in Eq. (15),  $P_{cr}$  depends on the size of the solution domain,  $N$ , because in the case of relatively small  $N$  only strongly self-trapped solitons, with sufficiently large  $P$ , may be narrow enough to fit into the domain. The *threshold* for the formation of the 2D solitons, i.e., the absolute minimum of  $P_{cr}$ , can be identified as  $P_{th} = P_{cr}(N \rightarrow \infty)$ . Fitting formulas displayed in Figs. 3(a)–3(c) help to identify the respective values of  $P_{th}$ .

The overall dependence of  $P_{th}$  on  $\sigma$  is displayed in Fig. 3(d). The increase of  $P_{th}$  with  $\sigma$  is naturally explained by the competition between the long-range self-attraction and contact self-repulsion at  $\sigma > 0$  (or insufficient self-attraction at  $\sigma < 0$ ).

The results summarized in Fig. 3 demonstrate that the QQI offers an advantage in comparison with the DDI for the formation of solitons, as the respective scaled formation threshold is considerably lower (roughly, by a factor of two) and, in addition to that, in the case of QQI the threshold is weakly affected by the competition with the contact nonlinearity, unlike the DDI model, where it is an important issue [6,8].

To further quantify the solitons, we define their effective area  $A_{eff}$  and structural anisotropy  $\mathcal{A}$  between the horizontal

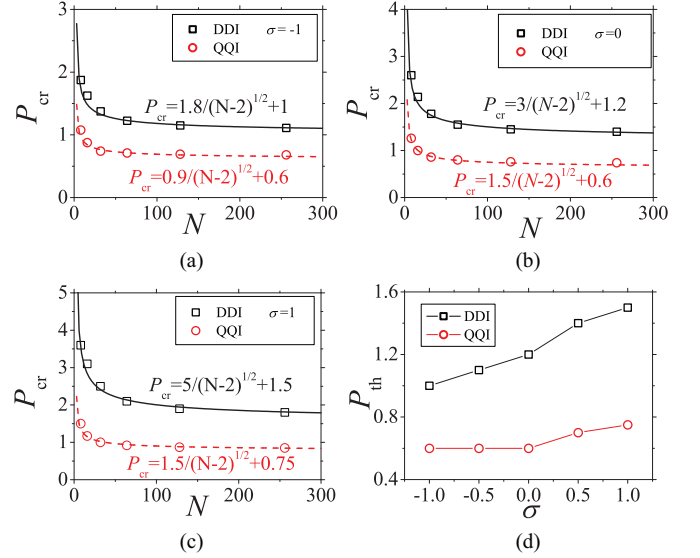


FIG. 3. (Color online) The minimum norm necessary for the formation of 2D discrete solitons,  $P_{cr}$ , under the action of the dipole-dipole (DDI) or quadrupole-quadrupole (QQI) interactions, as a function of the size of the solution domain  $N$ , for (a)  $\sigma = -1$ , the attractive-contact nonlinearity; (b)  $\sigma = 0$ , zero-contact nonlinearity; (c)  $\sigma = 1$ , repulsive-contact nonlinearity. Formulas written in the panels represent empiric fits to the plots to simple analytical expressions. (d) The threshold value of the norm, which corresponds to  $P_{cr}$  at  $N \rightarrow \infty$ , versus the strength of the contact nonlinearity.

(“hor”) and vertical (“vert”) directions as follows:

$$A_{eff} = \frac{(\sum_{m,n} |\phi_{mn}|^2)^2}{\sum_{m,n} |\phi_{mn}|^4}, \quad (21)$$

$$\mathcal{A} = \frac{|D_{hor} - D_{vert}|}{|D_{hor} + D_{vert}|}, \quad D_{hor} \equiv \frac{(\sum_m |\phi_{m,0}|^2)^2}{\sum_m |\phi_{m,0}|^4},$$

$$D_{vert} \equiv \frac{(\sum_n |\phi_{0,n}|^2)^2}{\sum_n |\phi_{0,n}|^4}, \quad (22)$$

where it is assumed that the soliton's center is fixed at site  $m = n = 0$ . In Figs. 4 and 5,  $A_{eff}$  and  $\mathcal{A}$  are plotted, along with the solitons' chemical potential, versus the *rescaled norm*, which is defined as

$$P^{res} \equiv P/P_{th}^{(QQ,DD)}, \quad (23)$$

where  $P_{th}^{(QQ,DD)}$  is taken, severally, from Fig. 3(d) as the respective threshold value for the QQI and DDI models.

Figures 4 and 5 demonstrate that the increase of the norm makes the solitons more tightly localized and more anisotropic, hence the long-range interactions QQI or DDI become dominant over the isotropic local interaction for “heavier” solitons. Furthermore, it is worth noting that  $\mu(P)$  dependencies in Fig. 6 satisfy the Vakhitov–Kolokolov criterion,  $d\mu/dP < 0$ , which is a well-known necessary stability condition for modes supported by self-attractive nonlinearities [87,89]. In particular, this is true in the case of  $\sigma = +1$ , when the attractive long-range interactions clearly beat the contact self-repulsion.

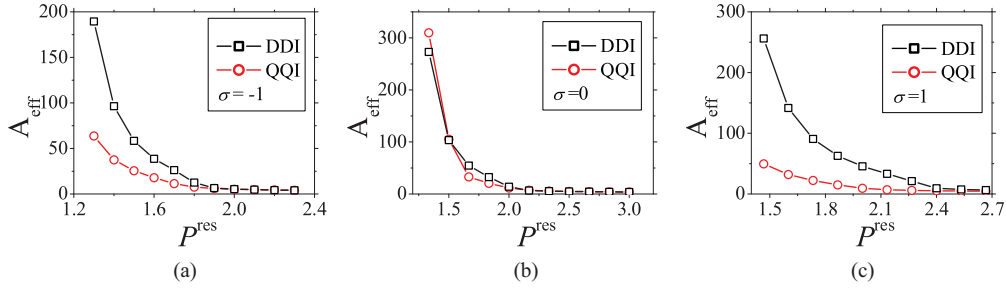


FIG. 4. (Color online) Effective area  $A_{\text{eff}}$  [see Eq. (21)] versus the rescaled norm [see Eq. (23)] for the solitons supported by the QQI and DDI in the combination with (a)  $\sigma = -1$ , (b)  $\sigma = 0$ , and (c)  $\sigma = 1$ , i.e., the attractive-, zero-, or repulsive-contact interactions. The numerical domain here is  $64 \times 64$ .

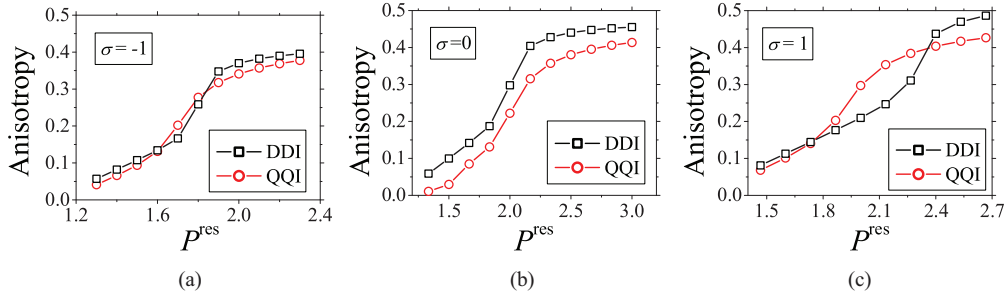


FIG. 5. (Color online) Same as in Fig. 4, but for anisotropy  $\mathcal{A}$ ; see Eq. (22).

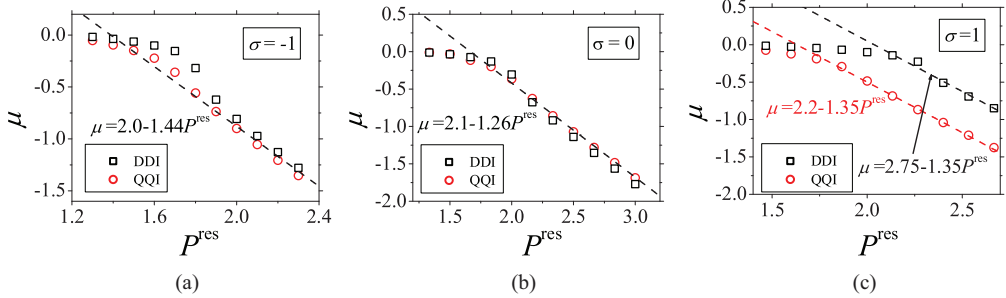


FIG. 6. (Color online) The same as in Figs. 4 and 5, but for chemical potential  $\mu$ ; see Eq. (20). The formulas present analytical fits for quasilinear portions of the  $\mu(P)$  dependencies.

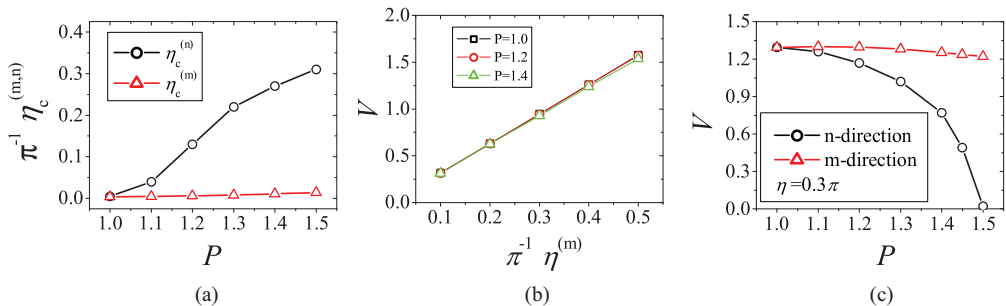


FIG. 7. (Color online) (a) Minimum size of kick necessary to set a soliton in motion in the horizontal and vertical directions ( $\eta_c^{(m)}$  and  $\eta_c^{(n)}$ , respectively), as a function of the soliton's norm  $P$ . (b) Velocity of the soliton moving in the horizontal direction versus the strength of the kick (at  $\eta > \eta_c^{(m)}$ ) for different fixed values of the norm. (c) Velocity of the soliton moving in the horizontal ( $m$ ) and vertical ( $n$ ) directions versus  $P$  for a fixed kick's strength,  $\eta = 0.3 > \eta_c^{(m,n)}$ .

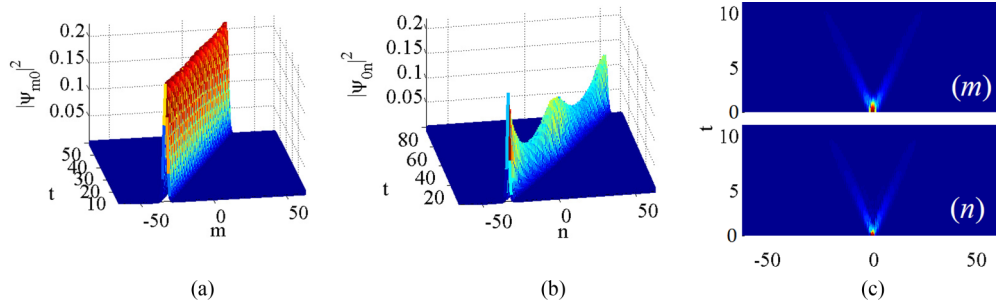


FIG. 8. (Color online) Evolution of a soliton with norm  $P = 1.2$  kicked with strength  $\eta = 0.4\pi$  in the (a)  $m$  (horizontal) direction and (b)  $n$  (vertical) direction. The evolution is displayed in cross sections ( $n = 0$ ) and ( $m = 0$ ), respectively. (c) Destruction of soliton by the staggering kick  $\eta = \pi$  applied in either direction.

#### IV. MOBILITY AND COLLISIONS OF THE DISCRETE SOLITONS

##### A. Setting the solitons in motion

Mobility of discrete solitons is a basic issue in the theory of nonlinear dynamical lattices [90]. In 2D lattices with the on-site (contact) nonlinearity, the mobility crucially depends of the type of the nonlinearity. The cubic on-site term, which corresponds to the critical collapse in the 2D continuum limit [87], gives rise to immobile discrete solitons strongly pinned to the underlying lattice. On the other hand, subcritical nonlinear terms, such as saturable [91] or quadratic [92], can readily create mobile 2D lattice solitons. In the 1D setting, it has been demonstrated that the DDI helps to enhance the mobility of discrete solitons [27,28]. The mobility and its consequences, such as collisions, were not studied previously on 2D lattices with long-range intersite interactions.

Here we focus on the mobility of 2D discrete solitons built solely by the long-range interactions (QQI), setting  $\sigma = 0$  in Eq. (15). Because the system is anisotropic, we separately consider the initiation of the soliton motion by kicks applied in the horizontal and vertical directions:

$$\psi_{mn}^{(\text{hor})}(t=0) = \phi_{mn} e^{i\eta m}, \quad \psi_{mn}^{(\text{vert})}(t=0) = \phi_{mn} e^{i\eta n}, \quad (24)$$

where  $\eta$  is the strength of the kick and  $\phi_{mn}$  is the stationary soliton solution [recall it is prolate in the horizontal ( $m$ ) direction; see Fig. 2].

Simulations demonstrate that, to set the solitons in the state of persistent motion, the kick must exceed a finite threshold value  $\eta_c$ . The kick with  $\eta < \eta_c$  may only shift the soliton from the initial position by a finite distance (i.e., the soliton starts to move but then comes to a halt). Figure 7(a) shows the threshold as a function of of the soliton's norm  $P$ . It is seen that the dependence is strongly anisotropic: the horizontal threshold  $\eta_c^{(m)}$  is very small and almost does not depend on  $P$ , while its vertical counterpart  $\eta_c^{(n)}$  is much larger and grows roughly linearly with  $P$ .

Obviously, the size of the kick in Eq. (24) is limited to  $\eta \leq \pi$ . In the limit case of  $\eta = \pi$ , the kick makes the soliton *staggered*, rather than moving, which results in destruction of the kicked soliton. Typical examples of the evolution of the kicked solitons are displayed in Fig. 8. In Fig. 8(a), the soliton moving in the horizontal direction is robust, while in Fig. 8(b) the same soliton, kicked with the same  $\eta$  but vertically, is moving in a strongly perturbed oscillatory state. The trend

to the destruction of the kicked soliton becomes apparent at  $\eta > \pi/2$ . The destruction in the case of  $\eta = \pi$  is shown in Fig. 8(c).

Dependencies of the velocity of the moving soliton on the kick's strength ( $\eta$ ) and direction ( $m$  or  $n$ : horizontal or vertical), and on the soliton's power ( $P$ ), are presented in Figs. 7(b) and 7(c). The former figure shows that, similar to the usual properties of nonlinear-Schrödinger solitons in a continuous medium, the velocity of the horizontally kicked soliton increases as a linear function of  $\eta$  (with an offset at  $V = 0$  corresponding to the threshold value  $\eta_c^{(m)}$ ) and practically does not depend on the norm. On the other hand, Fig. 7(c) demonstrates that velocity of the established motion in the vertical direction strongly depends on the soliton's norm; the heavier solitons being much less motile. Thus, the mobility of 2D solitons maintained by the QQI is strongly anisotropic.

##### B. Collision between moving solitons

The robust mobility of the 2D discrete solitons in the horizontal direction suggests studying collisions between them [93–95]. To this end, we simulated Eq. (15) with the input

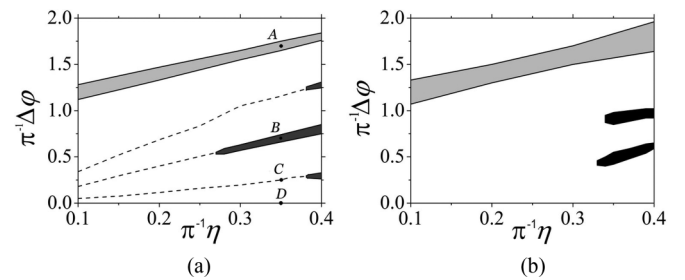


FIG. 9. (a) Plane of  $(\eta, \Delta\varphi)$  (with  $\eta \in [0.1\pi, 0.4\pi]$ ) for outcomes of collisions between lighter solitons, with  $P = 1.3$ . The merger and rebound occur in the white and light-gray areas, respectively (the symmetric merger is observed along the dashed lines). The colliding solitons destroy each other in the dark-gray area. Points A  $(\eta, \Delta\varphi) = (0.35, 1.7)\pi$ , B  $(\eta, \Delta\varphi) = (0.35, 0.7)\pi$ , C  $(\eta, \Delta\varphi) = (0.35, 0.25)\pi$ , and D  $(\eta, \Delta\varphi) = (0.35, 0)\pi$  represent typical examples of the full rebound, destruction, symmetric merger, and asymmetric merger, respectively. (b) The same plane for collisions between heavier solitons, with  $P = 1.8$ . The white and light-gray areas have the same meaning as in panel (a). Quasi-elastic collisions occur in the black regions.

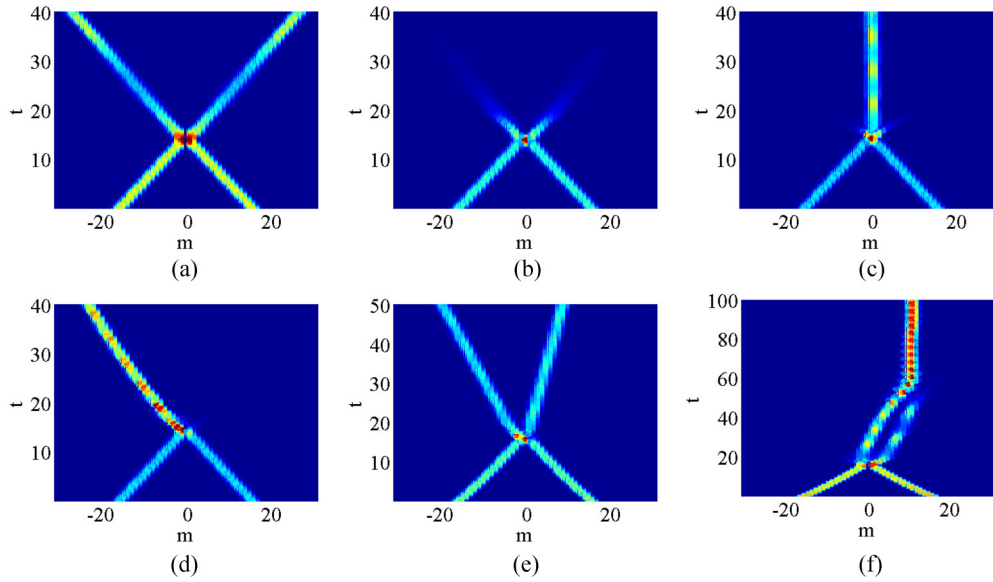


FIG. 10. (Color online) (a)–(d) Typical examples of collisions between solitons with norms  $P = 1.3$  (shown in the cross section  $n = 0$ ), corresponding to points A–D in Fig. 9(a). (e) An example of the quasi-elastic collision between heavier solitons, with  $P = 1.8$ , and  $(\eta, \Delta\varphi) = (0.35, 0.95)\pi$ . (f) An example of the multiple-rebound collision ending up with merger for  $P = 1.8$  and  $(\eta, \Delta\varphi) = (0.35, 1.58)\pi$ .

composed of two solitons separated by distance  $2m_0$ , i.e., with their centers placed at sites  $(\mp m_0, 0)$ , and phase shift  $\Delta\varphi$ , which is another control parameter of the collision, in addition to the relative velocity determined by kicks  $\pm\eta$  [93–96]:

$$\psi_{mn}(t=0) = \phi_{-m_0,0} e^{i\eta m} + \phi_{m_0,0} e^{-i\eta m + \Delta\varphi}. \quad (25)$$

In the simulations, the size of the domain was  $64 \times 64$ , with  $m_0 = 16$ . The norm of each soliton was  $P = 1.3$  or  $1.8$ , to explore the collision of relatively light and heavy solitons, respectively.

For  $P = 1.3$ , the moving solitons feature three major types of collisions in the plane of  $(\eta, \Delta\varphi)$ , as shown in Fig. 9(a): rebound, destruction, and merger. Particular examples of the rebound, destruction, symmetric merger, and asymmetric merger are displayed in Figs. 10(a)–10(d), which correspond, respectively, to sample points marked in Fig. 9(a): A  $(\eta, \Delta\varphi) = (0.35, 1.7)\pi$ , B  $(\eta, \Delta\varphi) = (0.35, 0.7)\pi$ , C  $(\eta, \Delta\varphi) = (0.35, 0.25)\pi$ , and D  $(\eta, \Delta\varphi) = (0.35, 0)\pi$ . Results of the direct simulations are displayed in cross section  $n = 0$ .

At larger values of the norm (here, at  $P = 1.8$ ), the moving solitons are more robust with respect to collisions. Namely, in this case destruction is not observed in the considered interval of the values of the kick,  $\eta \in [0.1\pi, 0.4\pi]$ , while a

new outcome occurs, in the form of quasi-elastic collisions [see Fig. 10(e)]. Parametric regions of three types of outcomes of collisions between heavier solitons; viz., the merger, rebound, and quasi-elastic interaction, are shown in Fig. 9(b), in the same plane as in Fig. 9(a). Because the merger and the rebound are quite similar to what was shown above for  $P = 1.3$ , here, in Fig. 10(e), we display only a typical example of the quasi-elastic collision. It is also worth noting that, in a parametric area close to the rebound [i.e., in the light-gray area in Fig. 9(b)], colliding solitons merge after multiple rebounds; see a typical example in Fig. 10(f).

Imbalance between powers (norms) of the colliding solitons,  $P_1 \neq P_2$ , also affects outcomes of the collisions; cf. Ref. [97]. For instance, the asymmetric merger of two solitons with equal powers,  $P_1 = P_2 = 1.3$ , which collide under the action of kicks  $\eta = \pm 0.35\pi$  with zero phase shift  $\Delta\varphi = 0$  displayed in Fig. 10(d) is replaced by mutual destruction for unequal powers  $P_1 = 1.0$ ,  $P_2 = 1.5$  (chosen so that the net power  $P_1 + P_2$  remains nearly the same as before), for nearly the same values of the kicks,  $\eta = \pm 0.40\pi$ , and again with  $\Delta\varphi = 0$ ; see Fig. 11(a). However, the reduction of the kick to  $\eta = \pm 0.20\pi$  switches the outcome of the collision for the same power-imbalance soliton pair from the destruction to

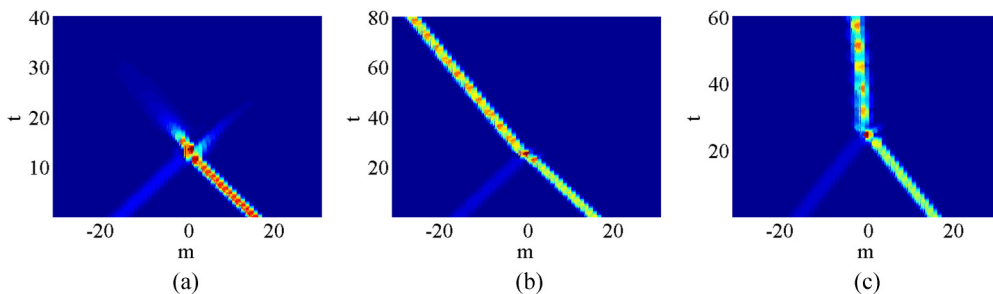


FIG. 11. (Color online) Outcomes of collisions between solitons with unequal total powers,  $P_1 = 1.0$  and  $P_2 = 1.5$ : (a) destruction, for kicks  $\eta = \pm 0.40\pi$  and phase shift  $\Delta\varphi = 0$ ; (b) merger, for  $\eta = 0.20\pi$  and  $\Delta\varphi = 0$ ; (c) also merger, for  $\eta = 0.20\pi$  and  $\Delta\varphi = 1.42\pi$ .

merger into a single moving soliton, as shown in Fig. 11(b), which is quite similar to the merger observed in Fig. 10(d). On the other hand, the symmetric collision leading to the merger of the solitons with  $P_1 = P_2 = 1.3$  into a single standing soliton, for  $\eta = \pm 0.35$  and  $\Delta\varphi = 0.20\pi$  in Fig. 10(c) extends, for  $P_1 = 1.0$ ,  $P_2 = 1.5$  and  $\eta = \pm 0.20\pi$ ,  $\Delta\varphi = 1.42\pi$ , into a similar merger, although this time the emerging single soliton is moving; see Fig. 11(c).

## V. CONCLUSIONS

The objective of this work is to study 2D matter-wave solitons in ultracold gas trapped in a deep an OL (optical-lattice) potential, with quadrupole-quadrupole interactions (QQIs) between particles. The quadrupoles are introduced as tight bound states of dipoles and antidipoles, whose polarizations are orientated in the  $z$  direction, i.e., perpendicular to the 2D plane in which the gas is trapped. The polarization of the quadrupoles is imposed by the dc electric field, which is also directed along  $z$ , but with the strength linearly growing along the  $x$  direction. Such a field configuration, which may be created by means of a tapered capacitor, is necessary because the quadrupoles interact locally with the gradient of the external field. The setting is described by the discrete (lattice) Gross-Pitaevskii equation, due to the fragmentation of the condensate by the strong OL. Together with the long-range QQI between lattice sites, the contact interaction, which may be either attractive or repulsive, is taken into account as the on-site nonlinearity in the resulting lattice model.

The shapes, stability, mobility, and collisions of 2D fundamental lattice solitons were studied by means of numerical simulations. It was found that stable solitons exist above a threshold value of the norm, which is lower than for matter-wave solitons in dipolar lattice-trapped gases. The threshold is much more weakly affected by the contact interactions than in the case of the DDI (dipole-dipole long-range interaction). The shape of the solitons features anisotropy, which is stronger for heavier solitons. The mobility of the discrete solitons on 2D lattices with long-range intersite interactions is studied here for the first time, also exhibiting strong anisotropy. Collision between mobile solitons were explored too. Collisions between lighter solitons may lead to their merger, rebound, and destruction. Heavier solitons are not destroyed by collisions. Estimates of physical parameters demonstrate that the proposed setting may be experimentally implemented in gases of small molecules, metastable alkaline-earth-metals, or alkaline diatoms.

A natural extension of the work may be to construct bound states of 2D lattice solitons. A challenging possibility is to look for topological 2D solitons, such as lattice vortices, in this discrete anisotropic system.

## ACKNOWLEDGMENTS

We appreciate valuable discussions with A. Maluckov. This work was supported by the Chinese agency CNNSF (Grants No. 11104083, No. 11204089, and No. 11205063), by the German-Israel Foundation through Grant No. I-1024-2.7/2009, and by the Tel Aviv University in the framework of the “matching” scheme for the postdoctoral fellowship of Y.L.

- 
- [1] L. P. Pitaevskii and A. Stringari, *Bose-Einstein Condensation* (Clarendon Press, Oxford, 2003).
  - [2] Ph. Courteille, R. S. Freeland, D. J. Heinzen, F. A. van Abeelen, and B. J. Verhaar, *Phys. Rev. Lett.* **81**, 69 (1998).
  - [3] S. Inouye, M. R. Andrews, J. Stenger, H.-J. Miesner, D. M. Stamper-Kurn, and W. Ketterle, *Nature (London)* **392**, 151 (1998).
  - [4] R. Heidemann, U. Raitzsch, V. Bendkowsky, B. Butscher, R. Löw, and T. Pfau, *Phys. Rev. Lett.* **100**, 033601 (2008).
  - [5] M. Viteau, M. G. Bason, J. Radogostowicz, N. Malossi, D. Ciampini, O. Morsch, and E. Arimondo, *Phys. Rev. Lett.* **107**, 060402 (2011).
  - [6] S. Giovanazzi, A. Görlitz, and T. Pfau, *Phys. Rev. Lett.* **89**, 130401 (2002).
  - [7] P. Pedri and L. Santos, *Phys. Rev. Lett.* **95**, 200404 (2005).
  - [8] T. Koch, T. Lahaye, J. Metz, B. Fröhlich, A. Griesmaier, and T. Pfau, *Nat. Phys.* **4**, 218 (2008).
  - [9] I. Tikhonenkov, B. A. Malomed, and A. Vardi, *Phys. Rev. Lett.* **100**, 090406 (2008).
  - [10] S. E. Pollack, D. Dries, M. Junker, Y. P. Chen, T. A. Corcovilos, and R. G. Hulet, *Phys. Rev. Lett.* **102**, 090402 (2009).
  - [11] T. Lahaye, C. Menotti, L. Santos, M. Lewenstein, and T. Pfau, *Rep. Prog. Phys.* **72**, 126401 (2009).
  - [12] A. Griesmaier, J. Werner, S. Hensler, J. Stuhler, and T. Pfau, *Phys. Rev. Lett.* **94**, 160401 (2005).
  - [13] M. Lu, N. Q. Burdick, S. H. Youn, and B. L. Lev, *Phys. Rev. Lett.* **107**, 190401 (2011).
  - [14] K. Aikawa, A. Frisch, M. Mark, S. Baier, A. Rietzler, R. Grimm, and F. Ferlaino, *Phys. Rev. Lett.* **108**, 210401 (2012).
  - [15] H. L. Bethlem, G. Berden, and G. Meijer, *Phys. Rev. Lett.* **83**, 1558 (1999).
  - [16] L. B. Hendrick, B. Giel, M. H. Floris, R. T. J. Cromptoets, J. A. V. R. André, and M. Gerard, *Nature (London)* **406**, 491 (2000).
  - [17] J. R. Bochinski, E. R. Hudson, H. J. Lewandowski, G. Meijer, and J. Ye, *Phys. Rev. Lett.* **91**, 243001 (2003).
  - [18] S. Giovanazzi, D. O’Dell, and G. Kurizki, *Phys. Rev. Lett.* **88**, 130402 (2002).
  - [19] D. L. Kovrizhin, V. G. Pai, and S. Sinha, *Europhys. Lett.* **72**, 162 (2005).
  - [20] V. M. Lashkin, *Phys. Rev. A* **75**, 043607 (2007).
  - [21] M. Vengalattore, S. R. Leslie, J. Guzman, and D. M. Stamper-Kurn, *Phys. Rev. Lett.* **100**, 170403 (2008).
  - [22] R. M. Wilson, S. Ronen, J. L. Bohn, and H. Pu, *Phys. Rev. Lett.* **100**, 245302 (2008).
  - [23] T. Lahaye, J. Metz, B. Fröhlich, T. Koch, M. Meister, A. Griesmaier, T. Pfau, H. Saito, Y. Kawaguchi, and M. Ueda, *Phys. Rev. Lett.* **101**, 080401 (2008).
  - [24] M. Fattori, G. Roati, B. Deissler, C. D’Errico, M. Zaccanti, M. Jona-Lasinio, L. Santos, M. Inguscio, and G. Modugno, *Phys. Rev. Lett.* **101**, 190405 (2008).



- [25] N. G. Parker and D. H. J. O'Dell, *Phys. Rev. A* **78**, 041601(R) (2008).
- [26] I. Tikhonenkov, B. A. Malomed, and A. Vardi, *Phys. Rev. A* **78**, 043614 (2008).
- [27] G. Gligorić, A. Maluckov, L. Hadžievski, and B. A. Malomed, *Phys. Rev. A* **78**, 063615 (2008).
- [28] Z. Luo, Y. Li, W. Pang, and Y. Liu, *J. Phys. Soc. Jpn.* **82**, 094401 (2013).
- [29] H. Saito, Y. Kawaguchi, and M. Ueda, *Phys. Rev. Lett.* **102**, 230403 (2009).
- [30] R. M. Wilson, S. Ronen, and J. L. Bohn, *Phys. Rev. A* **79**, 013621 (2009).
- [31] J. Cuevas, B. A. Malomed, P. G. Kevrekidis, and D. J. Frantzeskakis, *Phys. Rev. A* **79**, 053608 (2009).
- [32] G. Gligorić, A. Maluckov, L. Hadžievski, and B. A. Malomed, *Phys. Rev. A* **79**, 053609 (2009).
- [33] M. Klawunn and L. Santos, *Phys. Rev. A* **80**, 013611 (2009).
- [34] J. Metz, T. Lahaye, B. Fröhlich, A. Griesmaier, T. Pfau, H. Saito, Y. Kawaguchi, and M. Ueda, *New J. Phys.* **11**, 055032 (2009).
- [35] R. Nath and L. Santos, *Phys. Rev. A* **81**, 033626 (2010).
- [36] G. Gligorić, A. Maluckov, M. Stepić, L. Hadžievski, and B. A. Malomed, *Phys. Rev. A* **81**, 013633 (2010).
- [37] G. Gligorić, A. Maluckov, M. Stepić, L. Hadžievski, and B. A. Malomed, *J. Phys. B* **43**, 055303 (2010).
- [38] P. Muruganandam, R. K. Kumar, and S. K. Adhikari, *J. Phys. B* **43**, 205305 (2010).
- [39] R. M. W. van Bijnen, N. G. Parker, S. J. J. M. F. Kokkelmans, A. M. Martin, and D. H. J. O'Dell, *Phys. Rev. A* **82**, 033612 (2010).
- [40] M. Abad, M. Guilleumas, R. Mayol, M. Pi, and D. M. Jezek, *Phys. Rev. A* **81**, 043619 (2010).
- [41] G. Gligorić, A. Maluckov, M. Stepić, L. Hadžievski, and B. A. Malomed, *Phys. Rev. A* **82**, 033624 (2010).
- [42] K. Gawryluk, K. Bongs, and M. Brewczyk, *Phys. Rev. Lett.* **106**, 140403 (2011).
- [43] A. Bühler and H. P. Büchler, *Phys. Rev. A* **84**, 023607 (2011).
- [44] S. Müller, J. Billy, E. A. L. Henn, H. Kadau, A. Griesmaier, M. Jona-Lasinio, L. Santos, and T. Pfau, *Phys. Rev. A* **84**, 053601 (2011).
- [45] R. Eichler, J. Main, and G. Wunner, *Phys. Rev. A* **83**, 053604 (2011).
- [46] K. T. Xi, J. Li, and D. N. Shi, *Phys. Rev. A* **84**, 013619 (2011).
- [47] S. Rojas-Rojas, R. A. Vicencio, M. I. Molina, and F. Kh. Abdullaev, *Phys. Rev. A* **84**, 033621 (2011).
- [48] M. Abad, M. Guilleumas, R. Mayol, M. Pi, and D. M. Jezek, *Phys. Rev. A* **84**, 035601 (2011).
- [49] L. E. Young-S, P. Muruganandam, and S. K. Adhikari, *J. Phys. B* **44**, 101001 (2011).
- [50] P. Muruganandam and S. K. Adhikari, *J. Phys. B* **44**, 121001 (2011).
- [51] A. Maluckov, G. Gligorić, L. Hadžievski, B. A. Malomed, and T. Pfau, *Phys. Rev. Lett.* **108**, 140402 (2012).
- [52] M. Bauer and M. M. Parish, *Phys. Rev. Lett.* **108**, 255302 (2012).
- [53] D. Borzov, M. S. Mashayekhi, S. Zhang, J.-L. Song, and F. Zhou, *Phys. Rev. A* **85**, 023620 (2012).
- [54] K. Łakomy, R. Nath, and L. Santos, *Phys. Rev. A* **86**, 023620 (2012).
- [55] L. E. Young-S. and S. K. Adhikari, *Phys. Rev. A* **86**, 063611 (2012).
- [56] R. M. Wilson, C. Ticknor, J. L. Bohn, and E. Timmermans, *Phys. Rev. A* **86**, 033606 (2012).
- [57] F. K. Abdullaev and V. A. Brazhnyi, *J. Phys. B* **45**, 085301 (2012).
- [58] P. Muruganandam and S. K. Adhikari, *J. Phys. B* **45**, 045301 (2012).
- [59] A. Maluckov, G. Gligorić, L. Hadžievski, B. A. Malomed, and T. Pfau, *Phys. Rev. A* **87**, 023623 (2013).
- [60] J. Denschlag and J. Schmiedmayer, *Europhys. Lett.* **38**, 405 (1997).
- [61] H. Sakaguchi and B. A. Malomed, *Phys. Rev. A* **83**, 013607 (2011); **84**, 033616 (2011); **88**, 043638 (2013).
- [62] J. Denschlag, G. Umshaus, and J. Schmiedmayer, *Phys. Rev. Lett.* **81**, 737 (1998).
- [63] Y. Li, J. Liu, W. Pang, and B. A. Malomed, *Phys. Rev. A* **88**, 053630 (2013).
- [64] F. K. Abdullaev, A. Gammal, B. A. Malomed, and L. Tomio, *Phys. Rev. A* **87**, 063621 (2013).
- [65] Y. Kawaguchi and M. Ueda, *Phys. Rep.* **520**, 253 (2012).
- [66] A. D. Buckingham, R. L. Disch, and D. A. Dunmur, *J. Am. Chem. Soc.* **90**, 3104 (1968).
- [67] J. M. Junquera-Hernández, Sánchez-Marín, and D. Maynau, *Chem. Phys. Lett.* **359**, 343 (2002).
- [68] A. Derevianko, *Phys. Rev. Lett.* **87**, 023002 (2001).
- [69] R. Santra, K. V. Christ, and C. H. Greene, *Phys. Rev. A* **69**, 042510 (2004).
- [70] A. A. Buchachenko, *Eur. Phys. J. D* **61**, 291 (2011).
- [71] J. N. Byrd, R. Côté, and J. A. Montgomery, *J. Chem. Phys.* **135**, 244307 (2011).
- [72] S. G. Bhongale, L. Mathey, E. Zhao, S. F. Yelin, and M. Lemeshko, *Phys. Rev. Lett.* **110**, 155301 (2013); W.-M. Huang, M. Lahrz, and L. Mathey, [arXiv:1311.1947](https://arxiv.org/abs/1311.1947).
- [73] V. E. Lembessis and M. Babiker, *Phys. Rev. Lett.* **110**, 083002 (2013).
- [74] L. D. Landau and E. M. Lifshitz, *The Field Theory* (Nauka Publishers, Moscow, 1988).
- [75] A. R. Massih and G. A. Mansoori, *Fluid Phase Equilib.* **10**, 57 (1983).
- [76] O. Bang, W. Królikowski, J. Wyller, and J. J. Rasmussen, *Phys. Rev. E* **66**, 046619 (2002).
- [77] W. Królikowski, O. Bang, N. I. Nikolov, D. Neshev, J. Wyller, J. J. Rasmussen, and D. Edmundson, *J. Opt. B: Quantum Semiclassical Opt.* **6**, S288 (2004).
- [78] S. Skupin, O. Bang, D. Edmundson, and W. Królikowski, *Phys. Rev. E* **73**, 066603 (2006).
- [79] E. W. Laedke, K. H. Spatschek, and S. K. Turitsyn, *Phys. Rev. Lett.* **73**, 1055 (1994); *Nonlinearity* **7**, 205 (1994).
- [80] B. A. Malomed and P. G. Kevrekidis, *Phys. Rev. E* **64**, 026601 (2001); P. G. Kevrekidis, B. A. Malomed, Z. Chen, and D. J. Frantzeskakis, *ibid.* **70**, 056612 (2004).
- [81] P. D. Rasmussen, F. H. Bennet, D. N. Neshev, A. A. Sukhorukov, C. R. Rosberg, W. Królikowski, O. Bang, and Y. S. Kivshar, *Opt. Lett.* **34**, 295 (2009).
- [82] O. Bang, P. L. Christiansen, F. If, K. Ø. Rasmussen, and Y. B. Gaididei, *Phys. Rev. E* **49**, 4627 (1994).
- [83] M. L. Chiofalo, S. Succi, and M. P. Tosi, *Phys. Rev. E* **62**, 7438 (2000).
- [84] J. Yang and T. I. Lakoba, *Stud. Appl. Math.* **120**, 265 (2008).
- [85] J. Yang and T. I. Lakoba, *Stud. Appl. Math.* **118**, 153 (2007).
- [86] B. B. Baizakov and M. Salerno, *Phys. Rev. A* **69**, 013602 (2004).

- [87] L. Bergé, *Phys. Rep.* **303**, 259 (1998); E. A. Kuznetsov and F. Dias, *ibid.* **507**, 43 (2011).
- [88] B. B. Baizakov, B. A. Malomed, and M. Salerno, *Europhys. Lett.* **63**, 642 (2003); J. Yang and Z. H. Musslimani, *Opt. Lett.* **28**, 2094 (2003).
- [89] A. A. Kolokolov, *Radiophys. Quantum Electron.* **17**, 1016 (1974); *Izv. Vyssh. Uchebn. Zaved. Radiofiz.* **17**, 1332 (1974).
- [90] P. G. Kevrekidis, *The Discrete Nonlinear Schrödinger Equation: Mathematical Analysis, Numerical Computations, and Physical Perspectives* (Springer, Berlin and Heidelberg, 2009).
- [91] R. A. Vicencio and M. Johansson, *Phys. Rev. E* **73**, 046602 (2006).
- [92] H. Susanto, P. G. Kevrekidis, R. Carretero-González, B. A. Malomed, and D. J. Frantzeskakis, *Phys. Rev. Lett.* **99**, 214103 (2007).
- [93] I. E. Papacharalampous, P. G. Kevrekidis, B. A. Malomed, and D. J. Frantzeskakis, *Phys. Rev. E* **68**, 046604 (2003).
- [94] S. V. Dmitriev, P. G. Kevrekidis, B. A. Malomed, and D. J. Frantzeskakis, *Phys. Rev. E* **68**, 056603 (2003).
- [95] J. Meier, G. I. Stegeman, Y. Silberberg, R. Morandotti, and J. S. Aitchison, *Phys. Rev. Lett.* **93**, 093903 (2004).
- [96] L. Khaykovich and B. A. Malomed, *Phys. Rev. A* **74**, 023607 (2006).
- [97] O. Bang and P. D. Miller, *Opt. Lett.* **21**, 1105 (1996).